Biosensors and Bioelectronics 26 (2011) 3500–3504

Contents lists available at ScienceDirect

Biosensors and Bioelectronics

journal homepage: www.elsevier.com/locate/bios

In situ synthesis of palladium nanoparticle–graphene nanohybrids and their application in nonenzymatic glucose biosensors

Li-Min Lu [a], Hong-Bo Li [a], Fengli Qu [b,*], Xiao-Bing Zhang [a,*], Guo-Li Shen [a], Ru-Qin Yu [a]

[a] State Key Laboratory of Chemo/Biosensing & Chemometrics, College of Chemistry and Chemical Engineering, Hunan University, Changsha 410082, PR China
[b] Shandong Provincial Key Laboratory of Life-Organic Analysis, College of Chemistry and Chemical Engineering, Qufu Normal University, Qufu, Shandong 273165, PR China

ARTICLE INFO

Article history:
Received 19 October 2010
Received in revised form 6 January 2011
Accepted 24 January 2011
Available online 2 February 2011

Keywords:
Nonenzymatic sensor
Glucose
Graphene
Pd nanoparticles

ABSTRACT

A nonenzymatic electrochemical biosensor was developed for the detection of glucose based on an electrode modified with palladium nanoparticles (PdNPs)-functioned graphene (nafion–graphene). The palladium nanoparticle–graphene nanohybrids were synthesized using an in situ reduction process. Nafion–graphene was first assembled onto an electrode to chemically adsorb Pd^{2+}. And Pd^{2+} was subsequently reduced by hydrazine hydrate to form PdNPs in situ. Such a PdNPs–graphene nanohybrids-based electrode shows a very high electrochemical activity for electrocatalytic oxidation of glucose in alkaline medium. The proposed biosensor can be applied to the quantification of glucose with a wide linear range covering from 10 μM to 5 mM (R = 0.998) with a low detection limit of 1 μM. The experiment results also showed that the sensor exhibits good reproducibility and long-term stability, as well as high selectivity with no interference from other potential competing species.

1. Introduction

Development of fast and reliable methods for glucose detection is of considerable importance in many areas, such as clinical diagnostics, biotechnology, and the food industry (Kang et al., 2007). Electrochemical sensors based on the immobilization of glucose oxidase on various substrates have been the topics of the most previous studies on this subject. These enzymatic sensors showed good selectivity and high sensitivity for the detection of glucose. However, some inevitable drawbacks such as the chemical and thermal instabilities originated from the intrinsic nature of enzymes as well as the tedious fabrication procedures may limit their analytical applications (Salimi and Roushani, 2005; Katakis and Domínguez, 1995).

Direct electrocatalytic oxidation of glucose at nonenzymatic electrode seems to be an attractively alternative technique free from above-mentioned drawbacks. This kind of biosensor is based on the current response of glucose oxidation directly at the electrode surface, and the electrocatalytic activity of the electrode material is, therefore, the key factor that affects both the sensitivity and the selectivity for detection of glucose (Safavi et al., 2009). Various metallic Pt-based nanomaterials such as ordered Pt nanotube arrays (Yuan et al., 2005), nanoporous PtPb networks (Wang et al., 2008), PtPb nanowire arrays (Bai et al., 2008), PtIr nanomaterials (Hindle et al., 2008) and PtRu nanoparticles (Li et al., 2008a) have been explored as electrode materials to develop nonenzymatic sensors for glucose. Although these metallic Pt-based electrodes exhibited high elecrocatalytic activities towards direct oxidation of glucose, they suffered from surface fouling due to the chemical absorption of intermediates chloride ions, which resulted in poor operational stability of these biosensors. Palladium nanoparticles (PdNPs) is one of the most efficient catalysts in the formation of the C–C bond and chemical transformations such as hydrogenation, hydrodechlorination, carbonylation and oxidation (Lim et al., 2005). Several Palladium nanoparticles (Miao et al., 2009; Chen et al., 2010a) based enzyme-free biosensors have also been reported for glucose, which exhibited effectively improved sensitivity and selectivity towards the oxidation of glucose.

Graphene, a single layer of carbon atoms in a closely packed honeycomb two-dimensional lattice, has attracted considerable attention from both the experimental and the theoretical scientific communities in recent years (Geim and Novoselov, 2007; Li et al., 2008b). Due to the unique physical and chemical properties, such as high surface area, excellent conductivity, ease of functionalization and production, graphene provides an ideal platform to prepare functional nanomaterials for electronics, electric devices, and biosensors (Geim and Novoselov, 2007; Li et al., 2008c; Shao et al., 2010). In the past few years, increasing numbers of researches in this field have been devoted to the hybrid of graphene with polymer, oxide and metallic nanoparticles such as graphene/polymer nanocomposites, graphene/Pt nanoparticle sheets, graphene/ionic liquid, graphene oxide–MnO_2 and nitrogen-doped graphene (Vickery et al., 2009; Guo et al., 2010; Chen et al., 2010b; Wang et al., 2010). The hybridization of graphene

* Corresponding author. Tel.: +86 731 88821960.
E-mail address: xbzhang@hnu.edu.cn (X.-B. Zhang).

0956-5663/$ – see front matter © 2011 Elsevier B.V. All rights reserved.
doi:10.1016/j.bios.2011.01.033

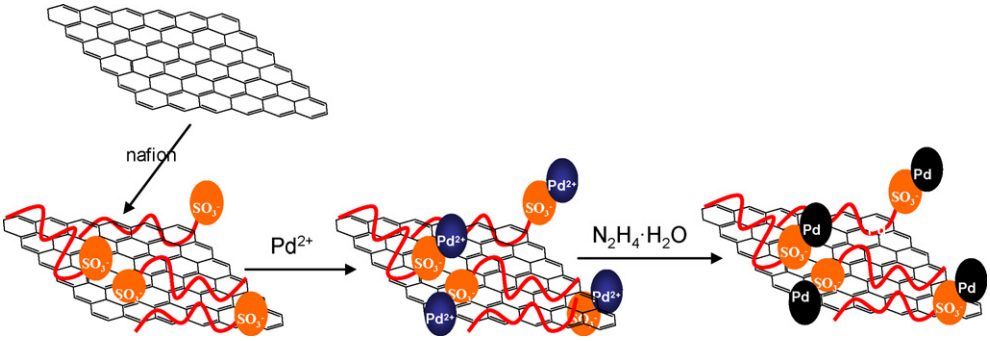

Scheme 1. The formation mechanism for nafion–graphene–Pd nanocomposites.

(or its derivatives) with functional nanomaterials might enhance the functional properties of each component, and even yield new properties via cooperative interaction.

The large surface area, high stability and excellent conductivity of the graphene together with the high electrocatalytic activity of PdNPs motivated us to synthesize PdNPs–graphene nanocomposites for fabricating of nonenzymatic glucose sensors. Herein, we report the in situ synthesis of palladium nanoparticle–graphene nanohybrids and their application in nonenzymatic glucose biosensors. The proposed nanohybrid-based electrode allows highly sensitive, stable, and fast amperometric sensing of glucose.

2. Experimental

2.1. Apparatus and reagents

Scanning electron microscopy (SEM) analysis was performed using a JSM-5600LV microscope (JEOL Ltd., Japan). Surface elemental composition of the synthesized samples was characterized by an energy-dispersive X-ray spectrometer (EDS). Transmission electron microscope (TEM) image was taken with a JEM-3010 transmission electron microscope (JEOL Co., Ltd., Japan). Atomic force microscopic (AFM) images were recorded with a Nanoscope IIIa scanning probe microscope (Digital Instruments, USA). The FT-IR spectra were recorded on a Nexus 670 FT-IR spectrophotometer (Nicolet Instruments) using a KBr disk at a resolution of 4 cm^{-1}. The cyclic voltammetric and amperometric measurements were carried out on a CHI 760B electrochemical workstation (Shanghai, China). A three-electrode cell (10 mL) was used with the modified glassy carbon (GC) electrode as the working electrode, a saturated calomel electrode (SCE) as the reference electrode and a platinum foil electrode as the counter electrode.

All potentials were measured versus the SCE, and all experiments were carried out at room temperature. $Pd(CH_3COO)_2$ and 5% nafion ethanol solution were purchased from Aldrich Chemical Co. (USA). D-(+)-Glucose was obtained from Merck. A 0.1 M NaOH solution was used as supporting electrolyte. All other reagents were of analytical grade, and doubly distilled water was used throughout the experiments.

2.2. Preparation of graphene composites

2.2.1. Preparation of graphene

Graphite oxide was obtained through natural graphite oxidation based on Hummer's method (Kovtyukhova et al., 1999). Generally, the preoxidized graphite powders were put into concentrated H_2SO_4 at 0 °C with gradual addition of $KMnO_4$ under stirring. The mixture was kept at 35 °C for several hours and diluted gradually in an ice bath with deionized water. The mixture was rediluted, followed by the addition of H_2O_2. The mixture was filtered when the color changed to brilliant yellow and washed with HCl aqueous solution and deionized water. The obtained graphite oxide powder was dialyzed in graphite oxide dispersion. The graphite oxide was exfoliated under sonication for about 2 h to ensure most graphite oxide was exfoliated to single layer graphene oxide. The obtained homogeneous yellow solution of single layer graphene oxide was reduced by hydrazine to remove the oxygenous groups. Black precipitates were washed and dried graphene, which were usually not soluble in water.

2.2.2. Preparation of graphene–nafion–PdNPs modified GC electrodes

A total of 1 mg of graphene was added to 1 mL of a 1 wt.% nafion–isopropyl-alcohol solution to form a homogeneous dispersion with mild ultrasonication. A volume of 5 μL of the resulting graphene–nafion solution was dropped onto a GC electrode and allowed to dry in ambient air for 24 h. Then the graphene–nafion modified GC electrode was soaked in 10 mM $Pd(CH_3COO)_2$ solution for 30 min. The resulted film was immersed into distilled water for 20 min to remove the uncoordinated Pd^{2+} ions. The Pd^{2+} ions in the graphene–nafion were reduced by dropping 20 μL of 2 mM hydrazine hydrate aqueous solution on the film for 30 min (Scheme 1).

3. Results and discussion

3.1. Characterization of graphene, nafion–graphene and the graphene–nafion–PdNPs nanocomposites

The morphology of graphene was characterized by TEM. As shown in Fig. S1a, the graphene presents nearly transparent flake-like shape with a length up to 1.5–2 μm and a width of ca. 0.8–1.2 μm. The AFM image of nafion–graphene is presented in Fig. S1b. The thickness of the nafion–graphene film was observed to be less than 60 nm.

FT-IR was also applied in examining graphene oxide and graphene. In the FT-IR spectrum of graphene oxide (Fig. S2), the bands around 3429, 1720, 1384, 1265, and 1060 cm^{-1} are attributed to the oxygen-containing functional groups on graphene oxide (Tang et al., 2009), confirming the successful oxidation of graphite. However, as shown in Fig. S1b, after the graphene oxide is chemically reduced, the characteristic absorption bands of oxide groups decreased dramatically, indicating that graphene oxide has been reduced to the graphene (Mermoux et al., 1991).

Direct morphological observation of the as-prepared PdNPs attachment to the surface of the graphene was made using a SEM. A typical SEM pictures is shown in Fig. 1A and B. We can find that many Pd dots grow on the surface of the graphene, in which there is a higher density of sulfonate groups. The average size of the dots was around 30–40 nm. Density calculations were performed by averaging data obtained from the AFM images (Fig. S3) of size

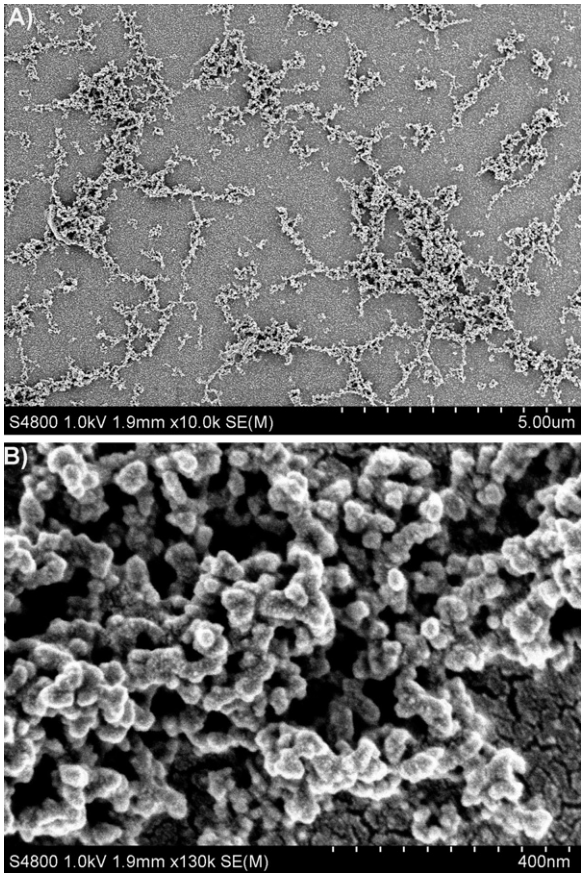

Fig. 1. (A) and (B) SEM images of the graphene–nafion–PdNPs nanocomposites with different amplified multiples.

2.5 μm × 2.5 μm. The average number of particles was calculated to be approximately 100 particles μm^{-2}. In order to further confirm the components, energy dispersive spectrum (EDS) analysis was performed (Fig. S4). It showed that the graphene–nafion–PdNPs nanocomposite was composed of C, Pd, S, F and O elements.

3.2. Electrochemical impedance spectroscopy (EIS) characterization of self-assembly process

In electrochemical impedance spectroscopy measurements, the semicircle diameter of impedance equals the electron transfer resistance (Ret), which controls the electron transfer kinetics of the redox probe at the electrode interface and is an important parameter. Fig. 2 presents the representative impedance spectrum of the bare GC electrode (a), nafion–GC electrode (b), nafion–graphene–GC electrode (c) and nafion–graphene–PdNPs-GC electrode (d) in 5.0 mM $K_3Fe(CN)_6/K_4Fe(CN)_6$ (1:1) containing 0.1 M KCl. The Nyquist semicircle of the nafion–GC electrode (curve b) increased dramatically compared with the bare GC electrode (curve a), which indicates that nafion film was an obstacle making the electron transfer of interface more difficult. After graphene assembled on the nafion film, the semicircle obviously decreased (curve c). Such decreased impedance may be ascribed to the conductivity of graphene. The immobilized of PdNPs (curve d) on the nafion–graphene–GC electrode made the semicircle decrease again.

3.3. Direct electrochemisty of modified electrodes

Fig. 3A shows cyclic voltammograms (CV) of nafion, nafion–graphene, nafion–PdNPs and nafion–graphene–PdNPs

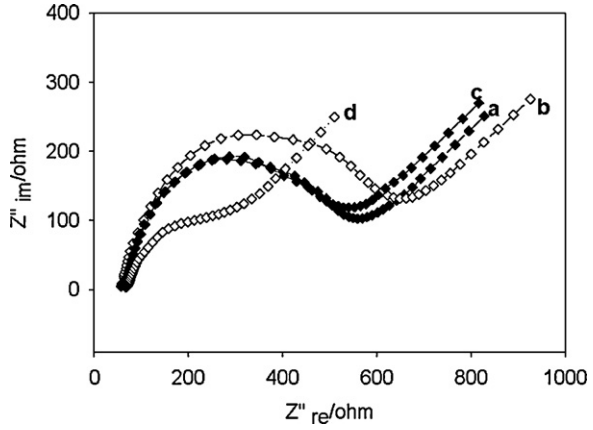

Fig. 2. The impedance spectrum of the bare GC electrode (a), nafion–GC electrode (b), nafion–graphene–GC electrode (c) and nafion–graphene–pd-GC electrode (d) in 5.0 mM $K_3Fe(CN)_6/K_4Fe(CN)_6$ (1:1) containing 0.1 M KCl.

modified GC electrodes in 0.1 M NaOH solution. Three redox peaks at the nafion–graphene–Pd modified electrode was obtained (Fig. 3A). The potential of 0 V was due to the formation of Pd–OH and a potential above +0.45 V corresponding with the metal oxide formation. The single cathodic peak at −0.45 V was related to the

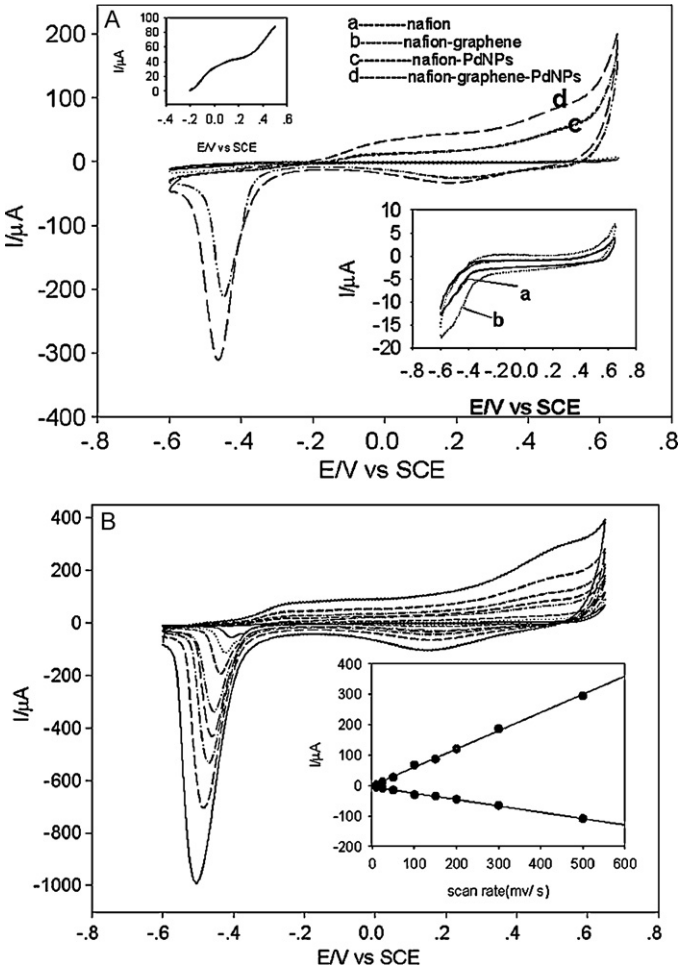

Fig. 3. (A) Cyclic voltammograms of nafion, nafion–graphene, nafion–Pd and nafion–graphene–Pd modified GC electrodes in 0.1 M NaOH solution; (B) cyclic voltammograms curves of nafion–graphene–Pd modified GC electrodes recorded in 0.1 M NaOH solution at different scan rates (inner to outer): 0.025, 0.05, 0.1, 0.2, 0.3, and 0.5 V s^{-1}; and peak current as a function of different scan rates (right inset).

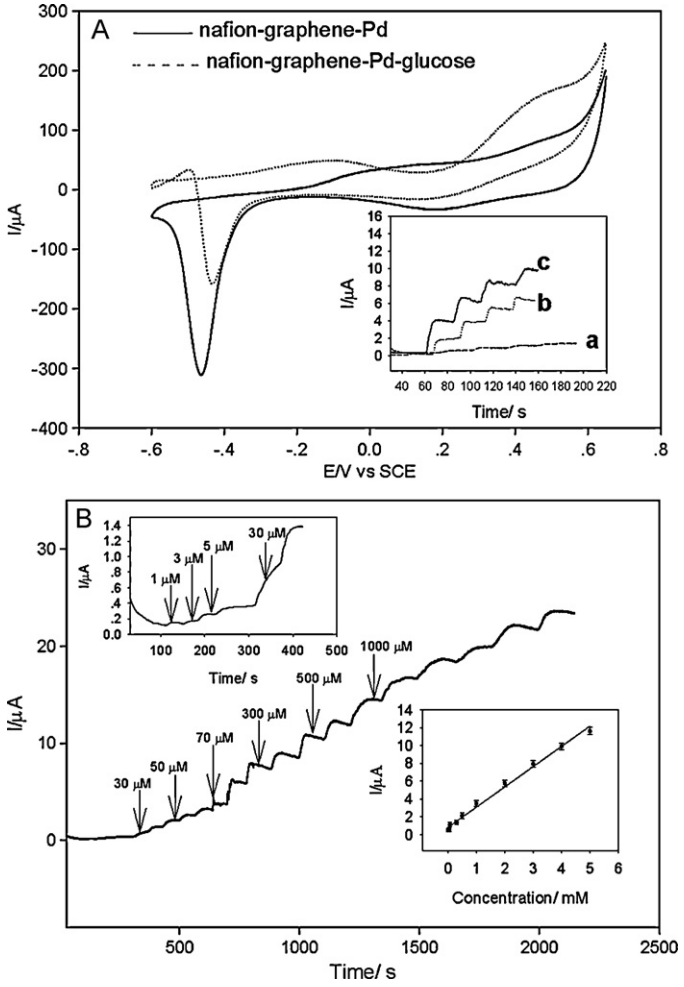

Fig. 4. (A) CV of the nafion–graphene–Pd without and with 4.0 mM glucose in 0.1 M NaOH at 100 mV s^{-1}. Inset: steady-state current–time response of various modified electrodes to 1 mM glucose at +0.4 V. (B) The typical current–time dynamic response of the nafion–graphene–Pd modified GC electrode towards various concentrations of glucose; left inset: amplified response curve, right inset: the calibration curve for glucose detection.

reduction of dissolved oxygen in solution (Chen et al., 2010a). The redox peak current of nafion–graphene–PdNPs is higher than that of nafion, nafion–graphene or nafion–PdNPs, which might be attributed to the synergistic effect of graphene and PdNPs. The cyclic voltammograms of nafion–graphene–PdNPs modified GC electrode at various scan rates were also investigated (Fig. 3B). The anodic or cathodic peak currents increased linearly as the scan rate grew from 25 to 500 mV s^{-1}, indicating that the electrochemical reaction in this composite film was a reversible and surface-confined process.

3.4. Electrocatalytic oxidation of glucose at the nafion–graphene–PdNPs modified GC electrode

The electrocatalytic activity of the nafion–graphene–PdNPs modified GC electrode towards glucose was investigated. Fig. 4A shows the CV of the nafion–graphene–PdNPs in 0.1 M NaOH between −0.6 V and +0.65 V with a scan rate of 100 mV s^{-1} in the presence and the absence of glucose, respectively. Upon the addition of glucose, a remarkable enhancement of the anodic current was observed, indicating that the nafion–graphene–PdNPs possess excellent electrocatalytic activity for glucose oxidation. The current of the oxidation peak achieved at +0.4 V for the nafion–graphene–PdNPs modified electrode is bigger than that obtained at −0.1 V, which might be a result of the incomplete oxidization of glucose under the potential of −0.1 V to form intermediates on the electrode surface and poison the active catalytic sites of the PdNPs (Chen et al., 2010b). Based on the previously reported oxidation mechanisms for glucose (Park et al., 2006; Safavi et al., 2009), a possible catalytic mechanism for the nafion–graphene–PdNPs modified electrode for glucose was proposed as following:

$$Pd + OH^- \rightarrow PdOH + e^-$$

$$PdOH + \text{glucose} \rightarrow Pd + \text{glucolactone}$$

Fig. 4A inset illustrates the response current of glucose by various modified electrodes at an applied potential of +0.4 V. The amperometric responses of nafion–graphene–PdNPs (c) modified GC electrode are larger than the summation of amperometric responses of the nafion–graphene (a) and nafion–PdNPs (b) modified GC electrode, which could be attributed to the synergistic reaction of PdNPs and graphene. The well-distributed PdNPs on the surface of graphene with a high density would provide more active sites for the catalytic redox reaction and greatly increase the electrocatalytic activity.

3.5. Amperometric sensing of glucose

The amperometric response of the nafion–graphene–PdNPs modified GC electrode to successive additions of glucose was further evaluated under the optimized experimental conditions. Fig. 4B shows the typical current–time dynamic response of the nafion–graphene–PdNPs modified GC electrode towards glucose. The electrode responded quickly to the change of glucose concentration and reaches about 95% of the steady-state current within 9 s, which was faster than those reported for Cu nanoparticle/SWCNT/Nafion modified glassy carbon electrode (10 s) (Male et al., 2004) and mesoporous platinum-modified platinum rod electrode (100 s) (Park et al., 2003). The amperometric signal shows linear correlation to glucose concentration in the range from 10 μM to 5 mM with a correlation coefficient of 0.998, which covers three orders of magnitude of glucose concentrations. It is much wider than that of nafion–PdNPs modified GC electrode (70 μM–5 mM) (this paper, Fig. S5), Copper nanocluster/MWCNT modified GC electrode (0.7–3.5 mM) (Kang et al., 2007) and electrospun Ni nanoparticle-loaded carbon nanofiber paste electrode (0.002–2.5 mM) (Liu et al., 2009). The detection limit was estimated to be 1 μM (based on S/N = 3) for glucose, which was lower than that of 10 μM at nafion–PdNPs modified GC electrode (this paper, Fig. S5), 8 μM at Pt–Pb nanowire array electrode (Bai et al., 2008), 25 μM at PtRu/MWCNTs modified GC electrode (Li et al., 2008a) and 2 μM at Ni powder modified electrode (You et al., 2003).

3.6. Interference study

Ascorbic acid (AA), uric acid (UA), and *p*-acetamidophenol (AP) present in physiological fluids are the most important interferences for direct electrochemical oxidation of glucose on different electrodes especially non-enzymatic sensors (You et al., 2003) (Yuan et al., 2005). The normal physiological level of glucose is about 3–8 mM, which is much higher than the concentrations of interfering species like AA (0.1 mM), UA (0.1 mM) and AP (0.1 mM). In the present work, we studied the interference effect of AA (0.1 mM), UA (0.1 mM) and AP (0.1 mM) on the amperometric response of 1 mM glucose and the response is shown in Table 1. As shown, the sensor showed excellent selectivity to glucose in the presence of AA, UA and AP.

Table 1
The interferences to glucose oxidation.

Substrate	Response current (μA)
Glucose (1 mM)	3.5
Ascorbic (0.1 mM)	0.081
Uric acid (0.1 mM)	~0
p-Acetamidophenol (0.1 mM)	~0

3.7. Stability and reproducibility of nafion–graphene–PdNPs modified GC electrode

The reproducibility and repeatability of the developed sensor were determined. In a series of 10 sensors prepared in the same way, a relative standard deviation of 3.7% was obtained towards 0.1 mM glucose, indicating the reliability of the method. A set of 10 different amperometric measurements for 0.1 mM glucose with a single sensor yield a R.S.D. of 3.4%.

The stability of the glucose sensor was explored. The proposed sensor was stored in air at ambient conditions. The response to 0.1 mM glucose was tested each week, after 35 days of storage, the response of the biosensor only decreased 2% compared to the initial response, which shows long-term stability.

3.8. Real sample analysis

To illustrate the feasibility of the nafion–graphene–PdNPs modified GC electrode in practical analysis, it is applied to detect glucose in human serum. 40.0 μL of serum sample was added in 10.0 mL of 0.1 M NaOH solution, and the current response at +0.40 V was recorded. The recovery of glucose was determined by standard addition of pure glucose to the solutions containing the serum samples and the corresponding results are given in Table S1. One can see that the nafion–graphene–PdNPs sensor gives good recoveries, indicating that potential interfering species in serum do not affect its detection of glucose.

4. Conclusion

The present work demonstrates that a nonenzymatic glucose sensor can be designed with PdNPs in situ formed within nafion–graphene film assembled on GC electrode. The PdNPs are confined in the nafion–graphene film. The sensor shows high electrocatalytic ability to glucose oxidation in alkaline solution and exhibits good linear dependence and selectivity to glucose concentration change, which would make the nafion–graphene–Pd glucose sensor more applicable in actual glucose detection.

Acknowledgments

This work was supported by the National Natural Science Foundation of China (21005047), Excellent Middle-age and Young Scientists Research Award Foundation of Shandong Province (BS2010SW012), National Natural Science Foundation of China (Grants J0830415, 20975034), “973” National Key Basic Research Program of China (Grants 2007CB310500, 2011CB911000), Program for Changjiang Scholars and Innovative Research Team in University, and Ministry of Education of China (Grant NCET-07-0272).

Appendix A. Supplementary data

Supplementary data associated with this article can be found, in the online version, at doi:10.1016/j.bios.2011.01.033.

References

Bai, Y., Sun, Y.Y., Sun, C.Q., 2008. Biosens. Bioelectron. 24, 579–585.
Chen, X.M., Lin, Z.J., Chen, D.J., Jia, T.T., Cai, Z.M., Wang, X.R., Chen, X., Chen, G.N., Oyama, M., 2010a. Biosens. Bioelectron. 25, 1803–1808.
Geim, A.K., Novoselov, K.S., 2007. Nat. Mater. 6, 183–191.
Guo, S.J., Dong, S.J., Wang, E.K., 2010. ACS Nano 4, 547–555.
Chen, S., Zhu, J.W., Wu, X.D., Han, Q.F., Wang, X., 2010b. ACS Nano 4, 2822–2830.
Hindle, P.H., Nigro, S., Asmussen, M., Chen, A., 2008. Electrochem. Commun. 10, 1438–1441.
Katakis, I., Domínguez, E., 1995. Trends Anal. Chem. 14, 310–319.
Kovtyukhova, N.I., Ollivier, P.J., Martin, B.R., Mallouk, T.E., Chizhik, S.A., Buzaneva, E.V., Gorchinskiy, A.D., 1999. Chem. Mater. 11, 771–778.
Kang, X.H., Mai, Z.B., Zou, X.Y., Cai, P.X., Mo, J.Y., 2007. Anal. Biochem. 363, 143–150.
Lim, S.H., Wei, J., Lin, J.Y., Li, Q.T., You, J.K., 2005. Biosens. Bioelectron. 20, 2341–2346.
Li, L., Zhang, W., Ye, J., 2008a. Electroanalysis 20, 2212–2216.
Li, D., Muller, M.B., Gilje, S., Kaner, R.B., Wallace, G.G., 2008b. Nat. Nanotechnol. 3, 101–105.
Li, X.L., Zhang, G.Y., Bai, X.D., Sun, X.M., Wang, X.R., Wang, E., Dai, H.J., 2008c. Nat. Nanotechnol. 3, 538–542.
Liu, Y., Teng, H., Hou, H.Q., You, T.Y., 2009. Biosens. Bioelectron. 24, 3329–3334.
Mermoux, M., Charbe, Y., Rousseau, A., 1991. Carbon 29, 469–474.
Malea, K.B., Hrapovic, S., Liu, Y.L., Wang, D.S., Luong, J.H.T., 2004. Anal. Chim. Acta 516, 35–41.
Miao, F.J., Tao, B.R., Sun, L., Liu, T., You, J.C., Wang, L.W., Chu, P.K., 2009. Sens. Actuators, B 141, 338–342.
Park, S., Chung, T.D., Kim, H.C., 2003. Anal. Chem. 75, 3046–3049.
Park, S., Boo, H.K., Chung, T.D., 2006. Anal. Chim. Acta 556, 46–57.
Salimi, A., Roushani, M., 2005. Electrochem. Commun. 7, 879–887.
Safavi, A., Maleki, N., Farjami, E., 2009. Biosens. Bioelectron. 24, 1655–1660.
Shao, Y.Y., Wang, J., Wu, H., Liu, J., Aksay, I.A., Lin, Y.H., 2010. Electroanalysis 22, 1027–1036.
Tang, L.H., Wang, Y., Li, Y.M., Feng, H.B., Lu, J., Li, J.H., 2009. Adv. Funct. Mater. 19, 1–9.
Vickery, J.L., Patil, A.J., Mann, S., 2009. Adv. Mater. 21, 2180–2184.
Wang, J., Thomas, D.F., Chen, A., 2008. Anal. Chem. 80, 997–1004.
Wang, Y., Shao, Y.Y., Matson, D.W., Li, J.H., Lin, Y.H., 2010. ACS Nano 4, 1790–1798.
You, T., Niwa, O., Chen, Z., Hayashi, K., Tomita, M., Hirono, S., 2003. Anal. Chem. 75, 5191–5196.
Yuan, J., Wang, K., Xia, X., 2005. Adv. Funct. Mater. 15, 803–809.